

# Comparison of the application value of spiral computed tomography and x-ray examination in the differential diagnosis of lung cancer and benign lung tumors

B. He<sup>1#</sup>, J. Xu<sup>2#</sup>, L. Wang<sup>1</sup>, B. Li<sup>1</sup>, X. Xu<sup>1\*</sup>

<sup>1</sup>Department of Radiology, the Affiliated Hospital of Shaoxing University (Shaoxing Municipal Hospital), Shaoxing 312000, Zhejiang Province, China

<sup>2</sup>Department of Radiology, Zhejiang Provincial People's Hospital, Hangzhou 310014, Zhejiang Province, China

## ABSTRACT

### ► Original article

**\*Corresponding author:**

Xinggang Xu, M.D.,

E-mail: 472184496@qq.com

Received: May 2024

Final revised: August 2024

Accepted: September 2024

Int. J. Radiat. Res., April 2025;  
23(2): 341-347

DOI: 10.61186/ijrr.23.2.12

**Keywords:** lung tumor, CT, X-ray, differential, diagnosis.

#These authors contributed equally to this work as co-first author.

**Background:** The differential diagnosis of lung cancer (LC) and benign lung tumors is challenging in clinic. Spiral computed tomography (CT) and X-ray are commonly utilized imaging techniques. Accordingly, the practical significance of CT and X-ray imaging in the differential identification of benign versus malignant pulmonary neoplasms was explored. **Materials and Methods:** A retrospective analysis was performed on data from 105 patients who had undergone both CT and X-ray examinations to evaluate variations in peripheral blood tumor markers. The imaging features of benign and malignant lung tumors were compared, and the diagnostic efficacy of CT and X-ray was assessed. **Results:** CT examination of patients with unilateral lung tumors or lung insufficiency demonstrated a greatly higher detection rate of speculated lesions compared to X-ray. Additionally, tumor markers showed a positive correlation with tumor size. The positive rate for differential diagnosis using CT was notably superior to that of X-ray ( $P < 0.05$ ). The sensitivity (Sen), specificity (Spe), accuracy (Acc), positive predictive value, and negative predictive value of CT and X-ray in differential diagnosis were 86.4%, 68.3%, 94.9%, 74.4%, 89.5%, 70.5%, 96.6%, 81.8%, 80.4%, and 58.0%, respectively. CT was considerably more valuable for differential diagnosis ( $P < 0.05$ ). **Conclusion:** X-ray and CT scans serve as pivotal diagnostic tools for distinguishing between benign and malignant pulmonary neoplasms. CT has a better effect in the differential diagnosis of lung tumors, and its imaging performance is more comprehensive, which is worthy of clinical application.

## INTRODUCTION

Among malignant tumors, lung cancer (LC) is characterized by a high incidence and often occult early onset, resulting in most patients presenting at an advanced stage by the time of treatment <sup>(1)</sup>. LC's incidence and mortality rates remain high. According to global cancer statistics for 2020, LC accounted for 11.4% of new cancer cases and 18% of cancer-related deaths <sup>(2)</sup>. Early-stage LC typically lacks obvious symptoms, and patients are frequently diagnosed incidentally during routine physical examinations or for other reasons <sup>(3)</sup>. Consequently, a significant proportion of LC patients are diagnosed at intermediate to advanced stages, missing the optimal window for surgical intervention. Statistics indicate that the 5-year survival rate for stage 0 LC patients who undergo surgery exceeds 90%, drops to over 60% for stage I, over 40% for stage II, and falls below 5% for stages III-IV <sup>(4)</sup>. The clinical manifestations of LC are diverse and depend on factors such as lesion location, pathological type, metastasis, and complications <sup>(5, 6)</sup>. Common symptoms include

persistent cough, hemoptysis, dyspnea, and weight loss, which often only appear in the later stages of the disease. As a result, early diagnosis based solely on clinical symptoms is challenging.

Molecular epidemiology, molecular biology, imaging, and endoscopic techniques can be utilized for the initial diagnosis of LC, with final confirmation typically provided by pathological examination <sup>(7)</sup>. Imaging methods such as chest X-ray, spiral CT, and positron emission tomography/computed tomography (PET/CT) offer detailed tumor images, aiding in the detection of pulmonary nodules and masses <sup>(8, 9)</sup>. Among these, chest X-ray is the most commonly employed preliminary screening tool, providing fundamental images of lung structures <sup>(10)</sup>. X-ray examination can reveal abnormal shadows or nodules in the lungs, providing some value for the early screening of LC. However, X-ray plain films have low resolution, limiting their ability to detect pulmonary nodules smaller than 1 cm and increasing the risk of missed or misdiagnosed cases <sup>(11)</sup>. In contrast, CT scanning technology offers high-resolution images of lung structures through

multi-slice imaging, allowing for clearer visualization of subtle lesions and nodule characteristics. CT can detect smaller nodules and evaluate their density, morphology, and location, aiding in the differentiation between benign and malignant lesions<sup>(12)</sup>. Compared to X-ray plain films, CT has higher sensitivity and specificity, making it a crucial tool for the early screening and diagnosis of LC<sup>(13)</sup>. Additionally, tumor markers can reflect the metabolic activity of tumor cells and are produced and secreted by these cells during cancer progression<sup>(14)</sup>. These markers can assist in distinguishing between benign and malignant tumors, monitoring recurrence, evaluating treatment efficacy, and assessing targeted therapies<sup>(15)</sup>.

This article aimed to enhance the efficacy of early screening for LC and benign tumors while reducing misdiagnosis and missed diagnosis rates. It presents a retrospective evaluation of the clinical performance of CT and X-ray imaging in differentiating between benign and malignant lung tumors, offering insights that could inform future investigations into the comparative utility of various radiological diagnostic methods for LC and lung tumor detection. By integrating modern imaging technologies with tumor marker detection, the study systematically assesses the ability of CT and X-ray to distinguish between these pulmonary conditions. This multi-faceted diagnostic approach not only improves the accuracy of early screening but also provides clinicians with a more comprehensive diagnostic foundation, thereby optimizing treatment plans. This contribution represents a novel and significant advancement in the existing literature, with substantial innovative and practical value.

## MATERIALS AND METHODS

### General information

The clinical data of 105 patients with lung tumors admitted to the Affiliated Hospital of Shaoxing University from June 2021 to December 2022 were retrospectively analyzed. The cohort included 62 men and 43 women, with a mean age of  $51.6 \pm 3.2$  years (range 41-75). Among these patients, 66 were diagnosed with LC via pathological examination or needle biopsy, comprising 41 men and 25 women, with a mean age of  $53.8 \pm 3.4$  years. The remaining 39 patients had benign tumors, including 21 men and 18 women, with a mean age of  $52.3 \pm 5.0$  years. Inclusion criteria: patients were diagnosed with LC or benign tumors, had no history of anti-tumor treatments such as chemotherapy, and underwent CT, X-ray, and serum tumor marker examinations prior to surgery. Additionally, patients with LC had no primary cancers at other sites. Exclusion criteria: patients with other serious organic diseases; severe malnutrition; pregnant or breastfeeding women; recent history of

bleeding or use of antiplatelet drugs; patients with acute or chronic infections, endocrine, metabolic, or other systemic diseases; and those with non-primary LC or other lung diseases. This experiment was approved by Ethics Committee of the Affiliated Hospital of Shaoxing University (under the title of "The diagnostic value of preoperative chest CT examination in clinical TNM staging of non-small cell lung cancer"; with registration number:2024(yan)-039-01 and registration date:2024.7.25).

### Tumor markers detection

Fasting venous blood of 3 mL was collected from all subjects. After anticoagulant treatment, serum was collected by centrifugation at 5,000 rpm/min for 10 min. CA125, CA153, CA199, CEA, NSE, and CAFRA21-1 antibodies (Nanjing Oukai Biotechnology Co., Ltd., China) were added. The levels of tumor markers CA125, CA153, CA199, CEA, NSE, and CYFRA21-1 in patients' serum were detected by electrochemiluminescence automatic immune analyzer (ARCHITECT i2000SR, Abbott, USA).

### Spiral CT scan

All patients underwent lung scanning with a CT scanner (Revolution CT, GE Healthcare, USA). The patient was placed in a supine position and scanned from apex to the base of lung under normal breathing. Slice thickness was 10 mm, pitch was 2 mm, current was 90-95 mA, and voltage was 110 kV. If a suspicious lesion was identified during the scan, 100 mL of 60% meglumine diatrizoate (Bayer Healthcare Co., Ltd. Guangzhou Branch, China) could be injected intravenously into the elbow, followed by a thin-slice scan of the suspicious lesion with a slice thickness of 3 mm and a pitch of 2 mm.

### X-ray scan

All patients underwent pulmonary X-ray examination with X-ray diagnostic instrument (DigitalDiagnost, Philips Medical System, the Netherlands). The patients were instructed to use supine position, and the side and front and rear chest were scanned under normal breathing condition. The X-ray parameters were set at a current of 50 mA and a voltage of 60-100 kV.

### Statistical methodologies

Patients were grouped regarding presence of benign or malignant lung tumors. Data analysis was performed using SPSS 19.0. Categorical data were denoted as frequency (%) and tested by chi-square test. Continuous data were presented as mean  $\pm$  standard deviation, with t-tests used for comparisons. Pearson correlation coefficient was used to evaluate the correlation between tumor markers and imaging results.  $P < 0.05$  indicates statistically significant differences.

RESULTS

Comparison of general data

Table 1 provides a comparative overview of the demographic and clinical characteristics distinguishing patients with benign and malignant lung tumors. The average age of patients with benign lung tumors was (52.3±5.0) years old. There were 21 male patients (53.8%) and 18 female patients (46.2%). The average disease duration was (7.5±1.3) months; The body mass index (BMI) was (23.4±2.8) kg/m<sup>2</sup>; The average age of patients with lung malignant tumors was (53.8±3.4) years old, including 41 male patients (62.1%) and 25 female patients (37.9%), with an average disease duration of (5.9±1.7) months; The BMI was (22.7±3.1) kg/m<sup>2</sup>. There was no obvious distinction in mean age, mean course of disease, body mass index (BMI), and sex ratio between benign and malignant lung tumor patients (P>0.05).

Table 1. Contrast of general data of patients.

Data	Benign tumor (n=39)	Malignant tumor (n=66)	P
Age (years)	52.3±5.0	53.8±3.4	0.171
Disease course (months)	7.5±1.3	5.9±1.7	0.212
BMI (kg/m <sup>2</sup> )	23.4±2.8	22.7±3.1	0.098
Gender [n(%)]			0.099
Male	21 (53.8)	41 (62.1)	
Female	18 (46.2)	25 (37.9)	

Note: BMI: body mass index

Contrast of peripheral blood tumor marker levels

The results of differences in CA125, CA153, CA199, CEA, NSE, and CYFR21-1 in peripheral blood of patients are illustrated in Figure 1. The levels of CA125, CA153, CA199, CEA, NSE, and CYFR21-1 in patients with malignant lung tumors were (212.3±33.2) U/mL, (178.2±24.6) U/mL, (134.3±23.8) U/mL, (156.2±30.2) µg/L, (121.7±13.2) µg/L, (132.1±16.5) µg/L, respectively; The levels of CA125, CA153, CA199, CEA, NSE, and CYFR21-1 in patients with benign lung tumors were (21.2±5.6) U/mL, (17.9±2.9) U/mL, (16.8±4.2) U/mL, (13.4±3.4) µg/L, (14.4±3.9) µg/L, and (15.7±5.2) µg/L, respectively. By comparison, CA125, CA153, CA199, CEA, NSE, and CYFR21-1 in peripheral blood of patients with malignant lung tumor were higher as against patients with benign lung tumor (P<0.05).

CT and X-ray imaging findings

The diagnostic imaging outcomes, as gleaned from CT and X-ray assessments, are delineated in figure 2. CT examination suggested 40 cases (38.1%) of unilateral or total lung atelectasis, 49 cases (46.7%) of spiculated and serrated lesions, 18 cases (17.1%) of peripheral solitary nodular lesions, 21 cases (20.0%) of irregular margin or lobulation sign, and 4 cases (3.8%) of other signs. X-ray films showed

unilateral or total atelectasis in 15 cases (14.3%), spiculated or serrated lesions in 24 cases (22.9%), peripheral solitary nodular lesions in 21 cases (20.0%), irregular margin or lobulation in 25 cases (23.8%), and others in 7 cases (6.7%). The proportion of unilateral or total atelectasis, burr and serrated imaging findings in CT examination was higher as against X-ray examination (P<0.05).

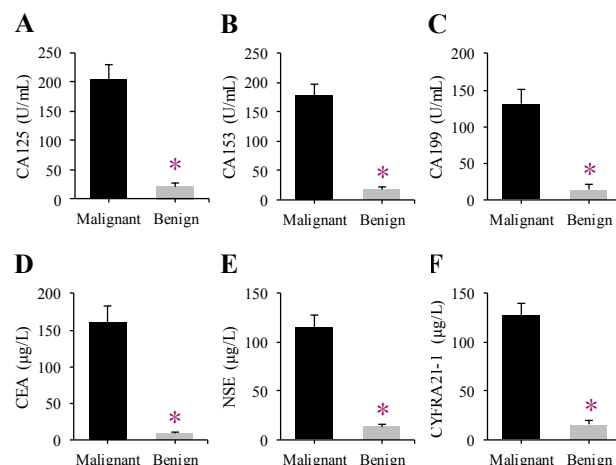


Figure 1. Contrast of peripheral blood tumor marker levels.

Note: A is CA125; B is CA153; C is CA199; D is CEA; E is NSE; F is CYFR21-1; \* indicates P<0.05 vs. LC group.

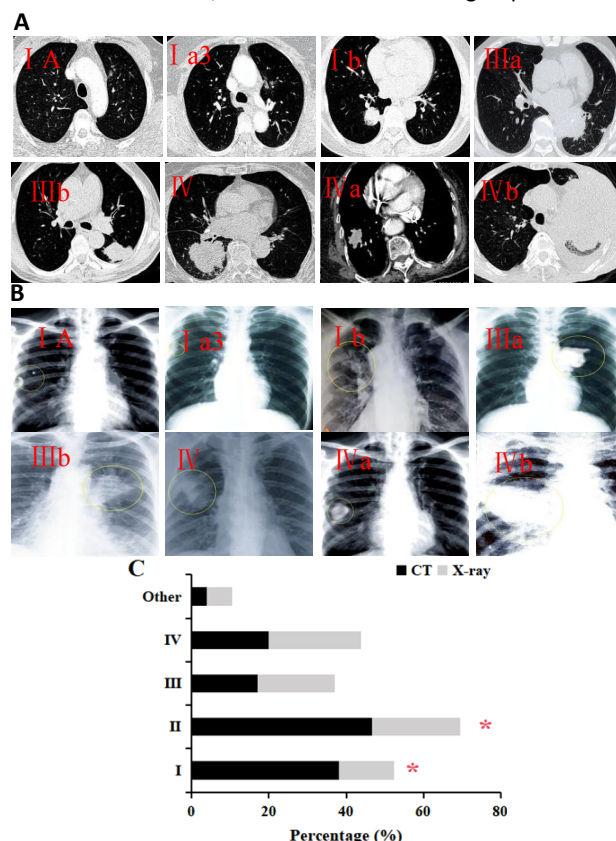
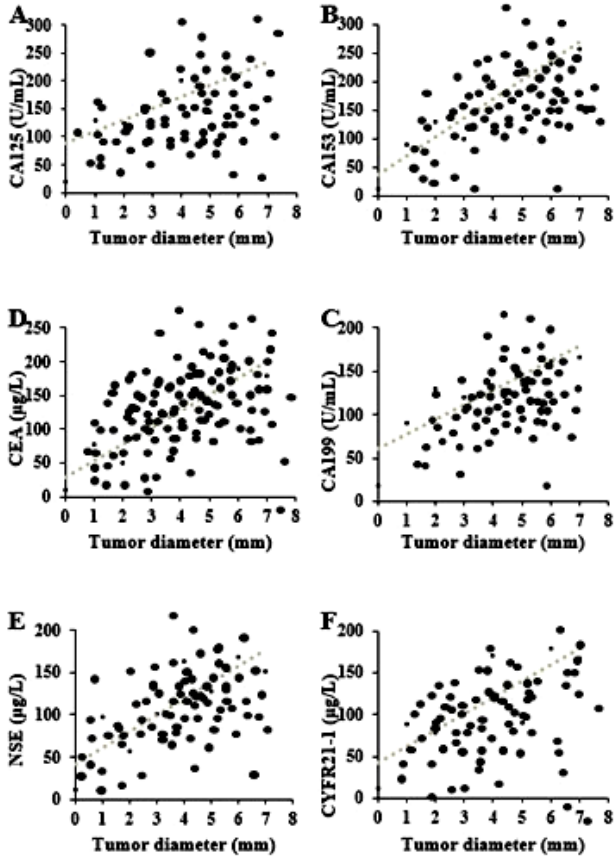


Figure 2. Contrast of the performance of different imaging examinations.

Note: A: CT images of LC at various stages; B: X-ray images of LC at different stages; C: distribution of different CT characteristics. I denotes unilateral lobe or whole lung atelectasis; II indicates burr or serrated signs; III represents peripheral solitary nodular lesions; IV shows irregular margins or lobulated signs; \* signifies P < 0.05 compared to CT imaging.

**Correlation analysis of tumor markers and CT scan results**

The correlation between CA125, CA153, CA199, CEA, NSE, and CYFR21-1 with tumor size in CT scan results was analyzed. The results showed that, CA125, CA153, CA199, CEA, NSE, and CYFR21-1 were notably positively correlated with tumor diameter ( $r=0.652, 0.534, 0.521, 0.568, 0.654, 0.692 P<0.01$ ) (figure 3).



**Figure 3.** Correlation between tumor markers and CT tumor size. (A: CA125; B: CA153; C: CA199; D: CEA; E: NSE; F: CYFR21-1).

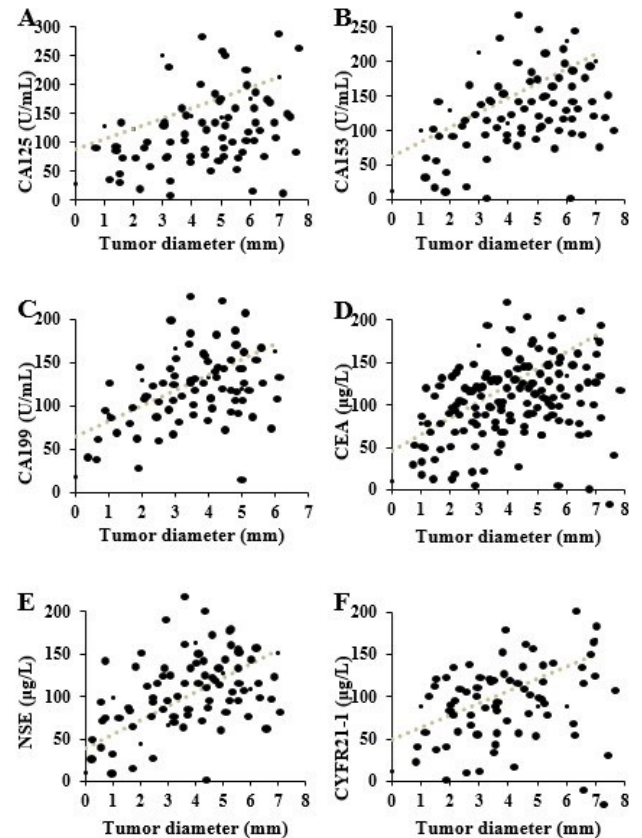
**Correlation analysis of tumor markers and X-ray scan results**

The article analyzed the correlation between CA125, CA153, CA199, CEA, NSE, and CYFR21-1 with tumor size in X-ray scanning results. The results showed that, CA125, CA153, CA199, CEA, NSE, and CYFR21-1 were notably positively correlated with tumor diameter ( $r=0.235, 0.205, 0.301, 0.212, 0.395, 0.303, P<0.05$ ) (figure 4).

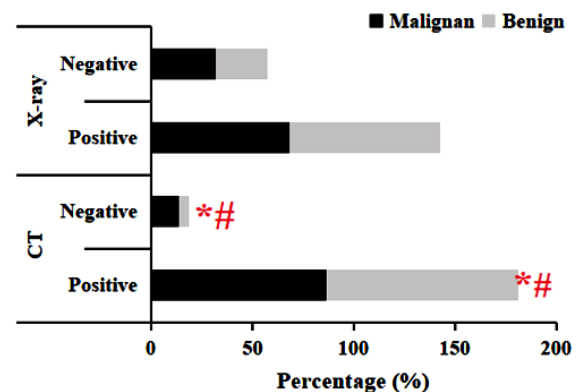
**Comparison of the clinical value of CT and X-ray in the diagnosis of pulmonary benign and malignant tumors**

Figure 5 presents a comparative illustration of the diagnostic findings derived from CT and X-ray imaging. In the CT results, 57 (86.4%) cases were positive and 9 (13.6%) cases were negative for malignant lung tumors. For benign lung tumors, 37 (94.9%) cases were positive and 2 (5.1%) cases were

negative. In the X-ray results, 45 (68.2%) cases were positive and 21 (31.8%) cases were negative for malignant lung tumors. For benign lung tumors, the diagnosis was positive in 29 (74.4%) cases and negative in 10 (25.6%) cases. The diagnostic efficiency of CT imaging was superior to that of X-ray ( $P<0.05$ ).



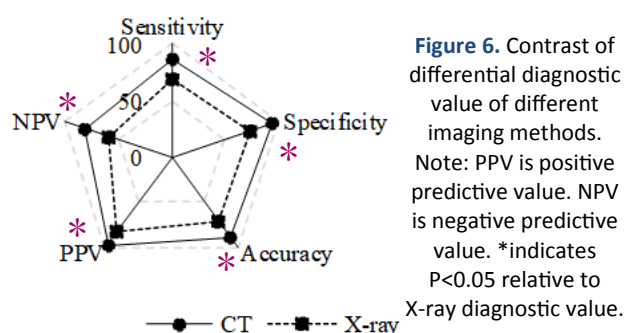
**Figure 4.** Correlation between tumor markers and X-ray tumor size. (A: CA125; B: CA153; C: CA199; D: CEA; E: NSE; F: CYFR21-1).



**Figure 5.** Differential diagnosis of different imaging modalities. Note: \*means  $P<0.05$  relative to X-ray diagnosis of LC; #indicates  $P<0.05$  compared with X-ray diagnosis of benign lung tumors.

The differences in Sen, Spe, Acc, positive predictive and negative predictive values between CT and X-ray images in differential diagnosis are shown in figure 6. The values of CT in the differential diagnosis were 86.4%, 94.9%, 89.5%, 96.6%, and

80.4%; those of X-ray diagnosis were 68.3%, 74.4%, 70.5%, 81.8%, and 58.0%, respectively. The values of CT in the differential diagnosis were higher as against X-ray ( $P < 0.05$ ).



## DISCUSSION

LC is the most common malignant tumor in clinical practice, characterized by rapid progression and high mortality, which poses a significant threat to patient health and life<sup>(16)</sup>. Early-stage LC often presents with subtle symptoms, leading most patients to be diagnosed at intermediate or advanced stages, thereby missing the optimal treatment window. Consequently, early screening and diagnosis are crucial for improving survival rates and patient outcomes. CT and chest X-ray are the primary radiological imaging methods used for early detection and diagnosis of LC and are widely implemented in clinical practice<sup>(17, 18)</sup>. The radiographic analyses of patients with pulmonary tumors, both benign and malignant, consistently revealed key findings such as unilateral or complete lung atelectasis, spiculated margins, the serrated sign, and peripheral solitary nodules with irregular or lobulated edges. Notably, pronounced disparities were observed in the manifestations of lung atelectasis, spiculated margins, and serrated signs. The utilization of CT scanning technology has been demonstrated to provide a clearer visualization of the extent of bronchial involvement in these patients. Furthermore, it enables a precise determination of the tumor's location, dimensions, shape, and margin characteristics<sup>(19)</sup>. During CT scan diagnosis of lung tumors, enhanced scanning with intravenous contrast agents can more precisely reveal the interior of suspicious lesions and their surrounding tissues<sup>(20, 21)</sup>. Additionally, CT diagnosis is not influenced by surrounding organs and soft tissues, allowing for the examination of small and hidden lesions, as well as assessing overall structure, shape, and involvement of bronchial and marginal areas, thus improving diagnostic accuracy<sup>(22)</sup>. Research confirmed that CT can identify mediastinal lymph node metastasis in patients with LC, which is crucial for optimizing treatment outcomes<sup>(23)</sup>.

Benign lung tumors are characterized by slow

growth rate, long course of disease, and inconspicuous clinical symptoms<sup>(24)</sup>. Early-stage LC often eludes detection on X-ray film, particularly in areas such as the lung apex, paraspinal regions, mediastinum, and the area posterior to the heart, leading to a high rate of missed diagnoses<sup>(25)</sup>. Comparative analysis has demonstrated that CT greatly outperforms X-ray film in the detection of both malignant and benign lung tumors, with superior measures of Acc, Sen, Spe, and predictive values. The X-ray imaging process involves the projection superposition of the entire lung's fluorescent screen, which results in lower image resolution and consequently hampers the identification and diagnostic efficacy for small lesions<sup>(26)</sup>. Compared with X-ray imaging, CT provides clearer visualization of the density distribution, lobulation patterns, contour features, calcifications, and other characteristics of benign lung tumors, thereby facilitating the effective differentiation between benign and malignant lesions<sup>(27, 28)</sup>. Furthermore, enhanced scanning of suspicious lesions allows for a more detailed examination of both the tumor and surrounding tissues, thereby improving the clinical diagnosis rate.

It was found that the levels of CA125, CA153, CA199, CEA, NSE, and CYFRA21-1 in peripheral blood of patients with malignant pulmonary neoplasms were visibly higher as against patients with benign pulmonary neoplasms, and there was an obvious correlation between the levels of tumor markers and tumor size measured by CT and X-ray. This correlation further indicates that the level of tumor markers can play an auxiliary role in clinical diagnosis and treatment. This is in line with the study of Pan *et al.* (2018)<sup>(29)</sup>. Studies have shown that tumor cells will release enzymes, hormones, and antigens when they die or grow and rupture, so tumor markers can also be used for the early diagnosis of LC<sup>(30)</sup>. CA125, CA153, and CA199 are common cancer screening items. CA125 is often used in the screening of ovarian tumors, endometrial cancer, pelvic inflammatory disease, and other diseases<sup>(31)</sup>. It was confirmed that CA125 levels are associated with LC stage, treatment efficacy, and recurrence, and can also aid in the auxiliary diagnosis of cancer cell metastasis<sup>(32)</sup>. CA153, primarily a breast cancer marker, is also useful in diagnosing pancreatic cancer, LC, ovarian cancer, and other conditions<sup>(33, 34)</sup>. CA199 serves as a marker for both lung and intestinal tumors<sup>(35)</sup>. CEA is a tumor marker frequently elevated in digestive tract tumors and can be applied in the diagnosis of malignant lung tumors<sup>(36)</sup>. NSE, an acid protease secreted by neurons and neuroendocrine cells, is a preferred marker for diagnosing SCLC and neuroblastoma<sup>(37)</sup>. Studies have indicated that the detection rate of NSE in patients with SCLC can range from 65% to 100%, making NSE a highly specific and sensitive marker for SCLC

diagnosis<sup>(38)</sup>. CYFRA21-1, a soluble fragment of cytokeratin 19, is a tumor marker with substantial relevance in LC diagnosis<sup>(39)</sup>. CA125, CA153, CA199, CEA, NSE, and CYFRA21-1 in the peripheral blood of patients with malignant lung tumors are notably higher than those in patients with benign lung tumors. The results further support the importance of tumor markers in the diagnosis of LC, and by combining with the imaging findings, the Acc and reliability of clinical diagnosis can be improved.

## CONCLUSION

In conclusion, through the comparative analysis of CT and X-ray in the differential diagnosis of parameters, peripheral blood tumor marker levels, etc., it can be clearly pointed out that the advantages of CT compared with X-ray in the differential diagnosis are mainly reflected in its higher Sen, Spe, and Acc, especially in showing the internal structure and boundary characteristics of tumors. Therefore, the application of CT should be paid more attention to and promoted in clinical practice.

## ACKNOWLEDGMENTS

*We sincerely thank all individuals and organizations for their support and help in the research process, special thanks to.*

**Funding:** Basic Public Welfare Program Projects from Science and Technology Bureau of Shaoxing: 2024A14015. Science and Technology Program Project from Health Commission of Shaoxing: 2023SKY082, 2024SKY075. General Research Project from Department of Education of Zhejiang Province: Y202454875.

**Conflict of interest:** The authors declare that there are no conflicts of interest related to this work.

**Ethical considerations:** This work has been approved by the relevant ethics committee of the Affiliated Hospital of Shaoxing University and strictly abided by the relevant ethical principles, laws, and regulations.

**Author contributions:** All authors had made significant contributions in experimental design, data collection, and analysis, as well as ensuring the scientific and reliable nature of the research.

## REFERENCES

- Gu M, Chen Z, Xiong H, Liu K, Ye Z, You Q (2022) Role and clinical significance of LncRNA16 in the malignant proliferation of lung cancer cells. *Cell Mol Biol*, **68**(7): 177-181. DOI: 10.14715/cmb/2022.68.7.29
- Wang W, Ma M, Li L, et al. (2022) MTA1-TJP1 interaction and its involvement in non-small cell lung cancer metastasis. *Transl Oncol*, **25**: 101500. DOI:10.1016/j.tranon.2022.101500
- Zhang S, Li D, Han X (2023) Systematic evaluation of clinical efficacy of CYP1B1 gene polymorphism in EGFR mutant non-small cell lung cancer observed by medical image. *Open Life Sci*, **18**(1):

20220688. DOI:10.1515/biol-2022-0688
- Bradley JD, Hu C, Komaki RR, et al. (2020) Long-term results of NRG Oncology RTOG 0617: Standard- versus high-dose chemoradiotherapy with or without cetuximab for unresectable stage III non-small-cell lung cancer. *J Clin Oncol*, **38**(7): 706-714. DOI:10.1200/JCO.19.01162
- He S, Li H, Cao M, et al. (2022) Survival of 7,311 lung cancer patients by pathological stage and histological classification: a multi-center hospital-based study in China. *Transl Lung Cancer Res*, **11**(8): 1591-1605. DOI:10.21037/tlcr-22-240
- Yu L, Zhang B, Zou H, et al. (2022) Multivariate analysis on development of lung adenocarcinoma lesion from solitary pulmonary nodule. *Contrast Media Mol Imaging*, **2022**: 8330111. DOI:10.1155/2022/8330111
- Kang Y, Lee SE, Kim CH, Lee YJ (2024) Revisiting the impact of clinicopathologic characteristics in PD-L1 profile in a large cohort of non-small cell lung cancer. *Transl Lung Cancer Res*, **13**(3): 475-490. DOI:10.21037/tlcr-23-812.
- Nooreldeen R and Bach H (2021) Current and future development in lung cancer diagnosis. *Int J Mol Sci*, **22**(16): 8661. DOI:10.3390/ijms22168661.
- Sullivan FM, Mair FS, Anderson W, et al. (2021) Earlier diagnosis of lung cancer in a randomised trial of an autoantibody blood test followed by imaging. *Eur Respir J*, **57**(1): 2000670. DOI:10.1183/13993003.00670-2020
- Robles-Zurita JA, McMeekin N, Sullivan F, Mair FS, Briggs A (2024) Health economic evaluation of lung cancer screening using a diagnostic blood test: The Early Detection of Cancer of the Lung Scotland (ECLS). *Curr Oncol*, **31**(6): 3546-3562. DOI:10.3390/currenol31060261
- Neshastehriz A, Hormozi-Moghaddam Z, Amini S, Taheri S, Abedi Kichi Z. (2024) Combined sonodynamic therapy and X-ray radiation with methylene blue and gold nanoparticles coated with apigenin: Impact on MCF7 cell viability. *Int J Radiat Res*, **22** (2): 509-513. DOI:10.52547/ijrr.21.24
- Chen L, Dong S, Chen Y, Tian L, He C, Tao S (2024) Diagnostic value of chest computed tomography scan based on artificial intelligence and deep learning in children with lobar pneumonia and analysis of image features before and after treatment: A retrospective cohort study. *Int J Radiat Res*, **22** (1): 199-205. DOI: 10.52547/ijrr.21.28
- Cao S and Shu Z (2024) Spectral CT based radiomics for predicting brain metastases in patients with lung cancer. *Int J Radiat Res*, **22** (2): 347-353. DOI:10.61186/ijrr.22.2.347
- Seijo LM, Peled N, Ajona D, et al. (2019) Biomarkers in lung cancer screening: achievements, promises, and challenges. *J Thorac Oncol*, **14**(3): 343-357. DOI:10.1016/j.jtho.2018.11.023.
- RM. Zhou, ZH. Cai, YR. Yuan, et al. (2024) Study on the application value of combined detection of multiple tumor markers in lung cancer classification diagnosis. *Int J Radiat Res*, **22** (2): 283-287. DOI:10.61186/ijrr.22.2.283
- Schabath MB and Cote ML (2019) Cancer progress and priorities: lung cancer. *Cancer Epidemiol Biomarkers Prev*, **28**(10): 1563-1579. DOI:10.1158/1055-9965.EPI-19-0221
- Godoy MCB, Lago EAD, Pria HRFD, Shroff GS, Strange CD, Truong MT (2022) Pearls and pitfalls in lung cancer CT screening. *Semin Ultrasound CT MR*, **43**(3): 246-256. DOI:10.1053/j.sult.2022.03.002
- Manapov F, Eze C, Holzgreve A, et al. (2022) PET/CT for target delineation of lung cancer before radiation therapy. *Semin Nucl Med*, **52**(6): 673-680. DOI:10.1053/j.semnuclmed.2022.05.003
- Al-Umairi R, Tarique U, Moineddin R, et al. (2022) CT patterns and serial CT changes in lung cancer patients post stereotactic body radiotherapy (SBRT). *Cancer Imaging*. **22**(1): 51. DOI:10.1186/s40644-022-00491-1
- Lee HY, Oh YL, Park SY (2021) Hyperattenuating adrenal lesions in lung cancer: biphasic CT with unenhanced and 1-min enhanced images reliably predicts benign lesions. *Eur Radiol*, **31**(8): 5948-5958. DOI:10.1007/s00330-020-07648-1
- Tamponi M, Crivelli P, Montella R, et al. (2021) Exploring the variability of radiomic features of lung cancer lesions on unenhanced and contrast-enhanced chest CT imaging. *Phys Med*, **82**: 321-331. DOI:10.1016/j.ejmp.2021.02.014.
- Luo C, Song Y, Liu Y, et al. (2022) Analysis of the value of enhanced CT combined with texture analysis in the differential diagnosis of pulmonary sclerosing pneumocytoma and atypical peripheral lung cancer: a feasibility study. *BMC Med Imaging*, **22**(1): 16. doi:10.1186/s12880-022-00745-1
- Larici AR, Franchi P, Del Ciello A, et al. (2021) Role of delayed phase contrast-enhanced CT in the intra-thoracic staging of non-

- small cell lung cancer (NSCLC): What does it add? *Eur J Radiol*, **144**: 109983. DOI:10.1016/j.ejrad.2021.109983
24. Bianconi F, Palumbo I, Fravolini ML, et al. (2022) Form factors as potential imaging biomarkers to differentiate benign vs. malignant lung lesions on CT scans. *Sensors*, **22**(13): 5044. DOI:10.3390/s22135044
  25. Bradley SH, Bhartia BS, Callister ME, et al. (2021) Chest X-ray sensitivity and lung cancer outcomes: a retrospective observational study. *Br J Gen Pract*, **71**(712): e862-e868. DOI:10.3399/bjgp.2020.1099
  26. Bradley SH, Hatton NLF, Aslam R, et al. (2021) Estimating lung cancer risk from chest X-ray and symptoms: a prospective cohort study. *Br J Gen Pract*, **71**(705): e280-e286. DOI:10.3399/bjgp20X713993
  27. Beck KS, Sung YE, Lee KY, Han DH (2020) Invasive mucinous adenocarcinoma of the lung: Serial CT findings, clinical features, and treatment and survival outcomes. *Thorac Cancer*, **11**(12): 3463-3472. DOI:10.1111/1759-7714.13674
  28. Sevillano D, Núñez LM, Chevalier M, García-Vicente F (2020) Definition of internal target volumes based on planar X-ray fluoroscopic images for lung and hepatic stereotactic body radiation therapy. Comparison to inhale/exhale CT technique. *J Appl Clin Med Phys*, **21**(8): 56-64. DOI:10.1002/acm2.12914
  29. Pan J, Zhou C, Zhao X, et al. (2018) A two-miRNA signature (miR-33a-5p and miR-128-3p) in whole blood as potential biomarker for early diagnosis of lung cancer. *Sci Rep*, **8**(1): 16699. DOI:10.1038/s41598-018-35139-3
  30. Osmani L, Askin F, Gabrielson E, Li QK (2018) Current WHO guidelines and the critical role of immunohistochemical markers in the subclassification of non-small cell lung carcinoma (NSCLC): Moving from targeted therapy to immunotherapy. *Semin Cancer Biol*, **52**(Pt 1): 103-109. DOI:10.1016/j.semcancer.2017.11.019.
  31. Du K, Li Q, Huang J, et al. (2024) An increase of serum CA-125 to two times of nadir level strongly predicts the image-identified relapse of serous ovarian cancer. *Sci Rep*, **14**(1): 14986. DOI:10.1038/s41598-024-65760-4
  32. Chen XK, Gu CL, Fan JQ, Zhang XM. (2020) P-STAT3 and IL-17 in tumor tissues enhances the prognostic value of CEA and CA125 in patients with lung adenocarcinoma. *Biomed Pharmacother*. **125**: 109871. DOI:10.1016/j.biopha.2020.109871
  33. Li G, Zhang H, Zhang L, et al. (2024) Serum Markers CA125, CA153, and CEA along with inflammatory cytokines in the early detection of lung cancer in high-risk populations. *Biomed Res Int*, **2024**: 9827549. DOI:10.1155/2022/1394042
  34. Li X, Xu Y, Zhang L (2019) Serum CA153 as biomarker for cancer and noncancer diseases. *Prog Mol Biol Transl Sci*, **162**: 265-276. DOI:10.1016/bs.pmbts.2019.01.005
  35. Jiang C, Zhao M, Hou S, et al. (2022) The indicative value of serum tumor markers for metastasis and stage of non-small cell lung cancer. *Cancers*, **14**(20): 5064. DOI:10.3390/cancers14205064
  36. Dal Bello MG, Filiberti RA, Alama A, et al. (2019) The role of CEA, CYFRA21-1 and NSE in monitoring tumor response to Nivolumab in advanced non-small cell lung cancer (NSCLC) patients. *J Transl Med*, **17**(1): 74. DOI:10.1186/s12967-019-1828-0
  37. Mao X, Liu J, Hu F, et al. (2022) Serum NSE is early marker of transformed neuroendocrine tumor after EGFR-TKI treatment of lung adenocarcinoma. *Cancer Manag Res*, **14**: 1293-1302. DOI:10.2147/CMAR.S349082
  38. Zhou W, Yang Y, Wang Z, Liu Y, Lari Najafi M (2023) Impact of HSP90 $\alpha$ , CEA, NSE, SCC, and CYFRA21-1 on lung cancer patients. *J Healthc Eng*, **2023**: 9796148. DOI:10.1155/2021/6929971
  39. Xi C, Jiang H, Xue Y, Lv Y, Wang C (2023) Effects of Bevacizumab combined with chemotherapy on CT, CyFRA21-1, and ProGRP and prognosis of lung cancer patients under nursing intervention. *Comput Math Methods Med*, **2023**: 9805719. doi:10.1155/2022/9422902.

